Biomedical Research and Therapy 2025, 12(8):7621-7632

Open Access Full Text Article

*Original Research*

# Transcriptome Analysis of the Protective Mechanism of Ectoine on Human Skin Keratinocytes

**Shuo Xu[1], Peixia Zhang[1], Lijuan Qiao[1,2,*], Guoping Shen[1], Yongchun Li[3], Derui Zhu[1,*]**

**ABSTRACT**

**Introduction**: Ectoine, a natural protective agent produced by halophilic bacteria, demonstrates remarkable skin-protective efficacy; however, the precise molecular mechanisms underlying its effects on skin cells remain poorly understood. This study investigated the differentially expressed genes (DEGs) in human keratinocytes (HaCaT) treated with ectoine to clarify its protective mechanisms. **Methods**: Cell viability was evaluated using the CCK-8 assay, identifying 0.2 mg/mL as the optimal ectoine concentration. A control group (C, 0 mg/mL) and an ectoine group (E, 0.2 mg/mL) were established. Flow cytometry quantified reactive oxygen species (ROS) and apoptosis. Illumina HiSeq RNA-seq identified DEGs; selected genes were validated by RT-qPCR. **Results**: Ectoine at 0.2 mg/mL increased cell viability to 134.0 % ± 3.2. Compared with the control group, ectoine significantly reduced the apoptosis rate and intracellular ROS levels ($P \leq 0.05$). RNA-seq (n = 3) identified 292 DEGs (87 up-regulated, 205 down-regulated). Among them, MMP25, NOXO1, ANGPTL4, and FoXO6—genes involved in oxidative stress, apoptosis, and proliferation—were markedly down-regulated, suggesting enhanced proliferation and anti-oxidative, anti-apoptotic effects. The cell-adhesion gene CNFN was significantly up-regulated, potentially reducing mechanical damage. **Conclusion**: Ectoine serves as a potent stabilizer and protectant, safeguarding skin by modulating genes that regulate oxidative stress, proliferation, and apoptosis.

**Key words:** Transcriptomics, Ectoine, HaCaT, CCK-8, FCM, Illumina HiSeq

## INTRODUCTION

Human keratinocyte cells (HaCaT), the primary cells of the skin epidermis, play a protective role by forming epidermal structures. When external factors such as dryness, radiation, wind, and temperature fluctuations accumulate, HaCaT cells are the first to be compromised, leading to skin dryness and aging-related damage [1].

Ectoine, a natural protectant synthesized by halophilic bacteria, shields these organisms from high-osmolarity environments [2]. It stabilizes cell membranes, nucleic acids, and proteins and lessens cellular stress caused by external factors [3–6], making it superior to other compatible solutes [7]. Recent studies show that ectoine binds water effectively and prevents transepidermal water loss [8]. For instance, Hseu *et al.* [9] reported that ectoine promotes skin whitening by inhibiting the ROS-p53/POMC-$\alpha$-MSH pathway in UV-irradiated HaCaT cells. Cheng *et al.* [10] used UVA- and $H_2O_2$-induced oxidation models of human skin fibroblasts and found that ectoine upregulated PI3K/AKT-related genes (COL1A1, COL1A2, FN1, IGF2, NR4A1, PIK3R1) and reduced intracellular ROS and malondialdehyde (MDA), thereby exerting protective effects. Moreover, ectoine alleviates atopic dermatitis and retinoid dermatitis caused by a weakened skin barrier [11]. However, the global genetic changes induced by ectoine in HaCaT cells remain unclear.

With the widespread adoption of high-throughput sequencing, transcriptomics has become a powerful tool for exploring quorum sensing, phenotypic shifts, metabolic adaptation, and key gene regulation. Lin *et al.* [12] showed that vitamin D markedly protects against skin photoaging; single-cell sequencing revealed that vitamin D downregulated inflammatory genes (Cd74, Cxcl2, Pcolce, Procr). RNA-seq data also demonstrated that ultraviolet A (UVA) activates Nrf2 and its targets—cyclin D1, TNFrsf1b, and Mybl1—producing antioxidant, anti-inflammatory, and anticancer effects in UVB-induced non-melanoma skin cancer (NMSC).

Therefore, we investigated the effects of ectoine on HaCaT cell viability, apoptosis, and intracellular ROS. We then applied transcriptomics to identify ectoine-induced genetic alterations and validated key findings with RT-qPCR. Our results show that ectoine promotes proliferation, inhibits apoptosis, and scavenges free radicals in HaCaT cells, pro-

[1]*Department of Basic Medical Sciences, Medical College, Qinghai University, Xining 810016, China*

[2]*College of Life Sciences, Northwest A&F University, Yangling, Shaanxi 712100, China*

[3]*School of Civil Engineering and Water Resources, Qinghai University, Xining, 810016, China*

**Correspondence**

**Lijuan Qiao**, Department of Basic Medical Sciences, Medical College, Qinghai University, Xining 810016, China

College of Life Sciences, Northwest A&F University, Yangling, Shaanxi 712100, China

Email: 2014980007@qhu.edu.cn

**Correspondence**

**Derui Zhu**, Department of Basic Medical Sciences, Medical College, Qinghai University, Xining 810016, China

Email: 2014980007@qhu.edu.cn

**Cite this article :** Xu S, Zhang P, Qiao L, Shen G, Li Y, Zhu D. **Transcriptome Analysis of the Protective Mechanism of Ectoine on Human Skin Keratinocytes**. *Biomed. Res. Ther.* 2025; 12(8):7621-7632.

**History**
- Received: 01-6-2025
- Accepted: 28-8-2025
- Published Online: 31-8-2025

**DOI : 10.15419/bhcnq037**



viding mechanistic insight and supporting its therapeutic application.

# METHODS

## Reagents and instruments

HaCaT cells were purchased from Wuxi Xinrun Biotechnology Co., Ltd. (Wuxi, China). Ectoine (≥98 %) was purchased from Shanghai Titan Scientific Co., Ltd. (Shanghai, China). Dulbecco's modified Eagle's medium (DMEM), TRIzol reagent, PrimeScript$^{TM}$ RT reagent kit with gDNA Eraser, and TB Green® Premix Ex Taq$^{TM}$ kit were obtained from TAKARA Holdings Inc. (Japan). Cell Counting Kit-8 was purchased from Elabscience Biotechnology Co., Ltd. (Wuhan, China). Annexin V-FITC Apoptosis Detection kit was purchased from TransGen Biotech Co., Ltd. (Beijing, China). The reactive oxygen species (ROS) test kit was purchased from Wuhan Servicebio Technology Co., Ltd. (Wuhan, China). An xMark microplate reader was bought from Bio-Rad Laboratories (USA). A $CO_2$ incubator (BPN-150CH) was purchased from Thermo Fisher Scientific (USA); a CytoFLEX flow cytometer was obtained from Beckman Coulter, Inc. (USA); and a LightCycler® 96 real-time PCR system was purchased from F. Hoffmann-La Roche Ltd. (Switzerland). Qubit 4.0 and NanoDrop 2000 spectrophotometers were manufactured by Thermo Fisher Scientific (USA). An Agilent 5300 Bioanalyzer was provided by Agilent Technologies Inc. (USA). A NovaSeq X Plus sequencer was purchased from Illumina, Inc. (USA).

## Cell culture

HaCaT cells were cultured in high-glucose DMEM supplemented with 10 % fetal bovine serum (FBS) and 1 % penicillin–streptomycin at 37 °C in 5 % $CO_2$. Cells were observed under an inverted microscope, and experiments were performed when confluence reached 90–95 %.

## Filtering the optimum concentration of ectoine

HaCaT cells were seeded into 96-well plates ($5 \times 10^3$ cells well$^{-1}$) and incubated for 24 h at 37 °C, 5 % $CO_2$. After washing with PBS, cells were treated with a concentration gradient of ectoine (0.05–0.50 mg mL$^{-1}$; n = 5 per group) for 24 h. Cell viability was assessed with the CCK-8 assay to determine the optimal ectoine concentration.

## Detecting apoptosis rate and intracellular ROS

HaCaT cells were seeded in 6-well Lab-Tek chambers with complete DMEM and grown to 80 % confluence. Cells were divided into a control group (C, 0 mg mL$^{-1}$) and an ectoine group (E, 0.20 mg mL$^{-1}$) (n = 3 per group). Cells were centrifuged at 1000 rpm for 5 min and washed with PBS. One aliquot was resuspended in 100 $\mu$L Annexin V Binding Buffer, supplemented with 5 $\mu$L Annexin V-FITC and 5 $\mu$L PI, and incubated for 15 min at room temperature in the dark. The remaining cells were incubated with 10 $\mu$mol L$^{-1}$ DCFH-DA in serum-free medium at 37 °C for 30 min in the dark. After two PBS washes, cells were filtered through a 300-mesh nylon membrane and analyzed on a flow cytometer to measure apoptosis and ROS levels.

## Library construction and quality control of transcriptome

Total RNA from groups C and E (n = 3 per group) was extracted using TRIzol, and integrity was verified on 1 % agarose gels. RNA purity ($OD_{260/280}$ = 1.8–2.2, $OD_{260/230} \geq 2.0$) and integrity (RIN ≥ 6.5, 28S:18S ≥ 1.0; >1 $\mu$g) were confirmed on a NanoDrop 2000 and Agilent 5300, respectively. Double-stranded cDNA was synthesized with the SuperScript kit and random hexamers, size-selected to ≈300 bp, and amplified by PCR. Strand-specific libraries were prepared, validated, and quantified on a Qubit 4.0 and sequenced on a NovaSeq X Plus. Adapter-containing reads, reads with >50% bases of Q ≤ 20, or containing undetermined bases were removed with fastp (v0.23.4) [13]. Clean reads were aligned to the reference genome using HISAT2 (v2.2.1) [14] and assembled with StringTie [15] .

## Differential expression analysis and functional enrichment

Transcripts per million reads (TPM) was estimated with RSEM [16]. Differential expression was analyzed with DESeq2 (v1.46.0) [17] or DEGseq (v1.26.0) [18]; genes with $|\log_2 FC| \geq 1$ and FDR ≤ 0.05 (DESeq2) or FDR ≤ 0.001 (DEGseq) were considered significantly differentially expressed. GO and KEGG enrichment were performed with GOATOOLS and KOBAS, respectively; terms with a Bonferroni-corrected P ≤ 0.05 were deemed significant [19].

## RT-qPCR validation of key DEGs

RNA samples meeting the above quality criteria (concentration > 5 ng $\mu$L$^{-1}$) were reverse-transcribed using the PrimeScript$^{TM}$ RT kit with

gDNA Eraser. The 20 $\mu$L reverse-transcription mix contained 10 $\mu$L Reaction I (5 × gDNA Eraser Buffer 2 $\mu$L, gDNA Eraser 1 $\mu$L, RNA + RNase-free $H_2O$ to 7 $\mu$L); incubation was 42 °C for 2 min. Reaction II (PrimeScript RT Enzyme Mix I 1 $\mu$L, RT Primer Mix 1 $\mu$L, 5 × PrimeScript Buffer 2 4 $\mu$L, RNase-free $H_2O$ 4 $\mu$L) was then added. cDNA was diluted 1:20 for qPCR. The 20 $\mu$L qPCR mix contained 10 $\mu$L TB Green Premix Ex Taq II, 0.8 $\mu$L each primer (10 $\mu$M), 2 $\mu$L cDNA, and 6.4 $\mu$L $H_2O$. Cycling: 95 °C 3 min; 45 cycles of 95 °C 10 s, 58 °C 20 s, 72 °C 30 s, with fluorescence acquisition during extension. PPIA served as the reference gene (n = 3 per group). Relative expression was calculated by the $2^{-\Delta\Delta Ct}$ method. Primers were synthesized by Sangon Biotech (**Table 1** ).

### Statistics

Statistical analyses were performed in GraphPad Prism 8. Normality was tested by the D'Agostino–Pearson omnibus test. Two-tailed Student's t-tests compared two groups, and one- or two-way ANOVA was used for ≥3 groups. Data are reported as mean ± SD (ns, not significant; $^{*}P < 0.05$; $^{**}P < 0.01$; $^{***}P < 0.001$; $^{****}P < 0.0001$).

## RESULTS

### Ectoine promoted the proliferation of HaCaT cells

Cell viability was assessed after treating HaCaT cells with different concentrations of ectoine. Results showed that cell viability increased as ectoine concentrations rose from 0.05 mg/mL to 0.20 mg/mL (103.94 ± 1.95 and 134.00 ± 3.22, respectively), and then declined as the concentration increased from 0.20 mg/mL to 0.50 mg/mL (107.10 ± 2.47; **Figure 1**). Overall, cell viability was significantly increased (>100 %) in all ectoine-treated groups (**Table S1**), indicating that ectoine may enhance the proliferation of HaCaT cells. Consequently, based on experimental results, 0.20 mg/mL was determined to be the optimal concentration for further experiments.

### Ectoine inhibited apoptosis and ROS generation in HaCaT cells

Apoptosis rates were analyzed using flow cytometry (**Figure 2ab**) after treating cells with 0.20 mg/mL ectoine. The apoptosis rate in the control group was 4.65 ± 0.57 %, whereas it was significantly lower in the ectoine-treated group (1.91 ± 0.19 %; **Table S2**). This suggests that ectoine may regulate HaCaT cell apoptosis by exerting anti-apoptotic effects. Intracellular reactive oxygen species (ROS) levels were measured using flow cytometry (**Figure 2 cd**). The relative DCFH-DA fluorescence intensity was significantly decreased in the ectoine-treated group, indicating a substantial reduction in intracellular ROS levels (**Table S3**). These findings demonstrate that ectoine effectively reduces endogenous ROS and minimizes oxidative stress.

### Transcriptome data processing and quality-control analysis

The raw data were filtered and screened to obtain more than 41,204,442 clean reads per group, with Q30 > 93.99 % and Q20 > 97.90 %. The error rate was <0.03 %, and the GC content ranged from 51.22 % to 52.79 % (**Table 2** ). Clean reads were aligned to the reference genome, and the mapping rates were statistically analyzed. Total mapping ranged from 97.39 % to 97.55 %, including a single-match rate >93.40 % and a multi-match rate of 3.03–4.10 %. These results indicate that the sequencing data were reliably processed and are qualified for subsequent analyses.

### Analysis of gene expression in response to ectoine

The expression levels of DEGs in the control (C) and ectoine (E) groups, measured as log2(FPKM + 1), were subjected to hierarchical clustering. Ectoine reversed the transcriptional differences observed between the C and E groups: clusters with low expression in the C group shifted to high expression in the E group, whereas clusters with high expression in the C group became low in the E group. More low-expression than high-expression clusters were observed in the E group, suggesting that ectoine primarily suppresses overall gene expression in HaCaT cells (**Figure 3a**). Differential-expression analysis (log2 fold-change $\neq 0$, $P \leq 0.05$) identified 292 DEGs between C and E, including 87 up-regulated and 205 down-regulated genes (**Figure 3b**).

### GO and KEGG functional annotation analysis of differential genes

DEGs between the C and E groups were annotated using the Gene Ontology (GO) database. In total, 292 DEGs were enriched in 43 GO terms. The top 20 enriched terms fell into three categories—biological process (BP), cellular component (CC), and molecular function (MF; **Figure 4a**). Within BPs, DEGs were mainly enriched in cellular processes, biological regulation, and metabolic processes. For CCs,

**Table 1: Primer sequences and product size**

| Genes name | Primer sequences (5'→3') | Length (bp) |
|---|---|---|
| ANGPTL4 | F: GAGGCTGGACAGTAATTCAGA, R:CGTGATGCTATGCACCTTCT | 134 |
| MMP25 | F: GACTGGCTGACTCGCTATGG, R:TGATGGCATCGCGCAACTT | 88 |
| NOXO1 | F: ATTCAGGCAGCTCAAGACCC, R:TGACCGAGAAGCTTTGGGAG | 93 |
| CNFN | F: TTGCTCCTCTGTGCCTTGCC, R:ACGGAGCCCTGGATGTGGT | 130 |
| FoxO6 | F: GTGGGGGAACCTTTCCTACG, R:TTCTGCACGCGGATGAACC | 207 |
| PPIA | F: GTCAACCCCACCGTGTTCTT, R:GTCAACCCCACCGTGTTCTT | 97 |

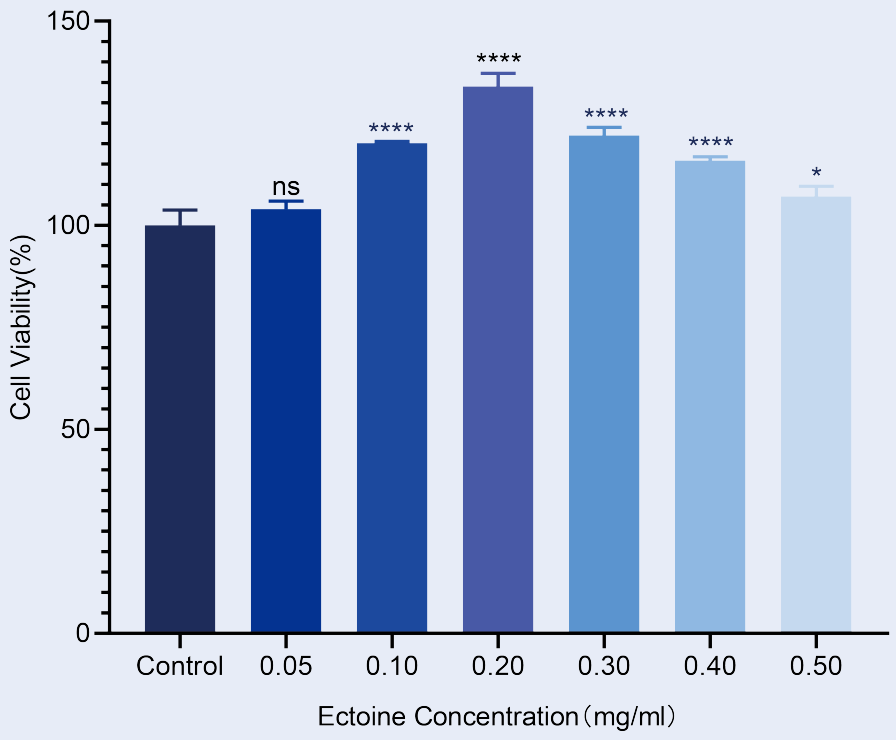


**Figure 1: Effect of different concentrations of ectoine on the viability of HaCaT cells.** Error bars indicate the standard deviation of three parallel samples. *: *P*-value < 0.05; **: *P*-value <0.01; ***: *P*-value <0.001; and ****: *P*-value <0.0001. Data were presented as means ± SD. **Abbreviations**: HaCaT (Human Keratinocytes Cells), SD (Standard Deviation)

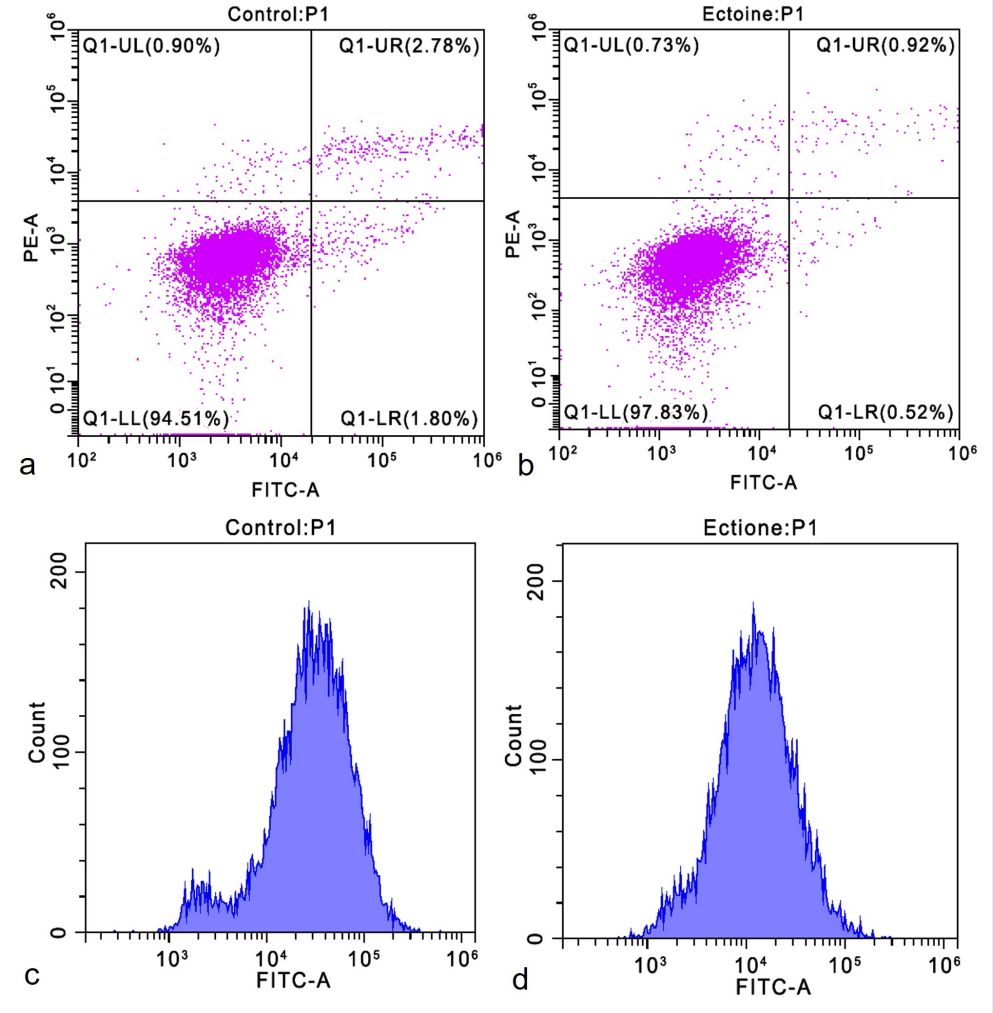


**Figure 2**: **Apoptosis rate and intracellular ROS level of HaCaT cells**. Apoptosis rate of cells treated with 0 mg/ml ectoine for 24 h (**a**). The apoptosis rate of cells treated with 0.20 mg/ml ectoine for 24 h (**b**). The intracellular ROS level in cells treated with 0 mg/ml ectoine for 24 h (**c**). The intracellular ROS level in cells treated with 0.20 mg/ml ectoine for 24 h (**d**). **Abbreviations**: HaCaT (Human Keratinocytes Cells), ROS (Reactive Oxygen Species)

**Table 2**: **Filtered data and quality statistics**

| Sampl | Raw reads | Clean reads | Q20 (%) | Q30 (%) | GC (%) | Total mapped | Multiple mapped | Unique mapped |
|---|---|---|---|---|---|---|---|---|
| C1 | 47683022 | 47205576 | 98.02 | 94.29 | 52.36 | 97.48% | 3.03% | 94.45% |
| C2 | 43301474 | 42862366 | 97.9 | 93.99 | 51.9 | 97.39% | 3.07% | 94.32% |
| C3 | 53243942 | 52725454 | 97.97 | 94.17 | 52.79 | 97.55% | 3.33% | 94.22% |
| E1 | 41565756 | 41204442 | 97.99 | 94.21 | 51.05 | 97.53% | 3.47% | 94.06% |
| E2 | 46817134 | 46392670 | 98.05 | 94.4 | 51.49 | 97.52% | 3.44% | 94.09% |
| E3 | 52862954 | 52385586 | 98.08 | 94.45 | 51.22 | 97.50% | 4.10% | 93.40% |

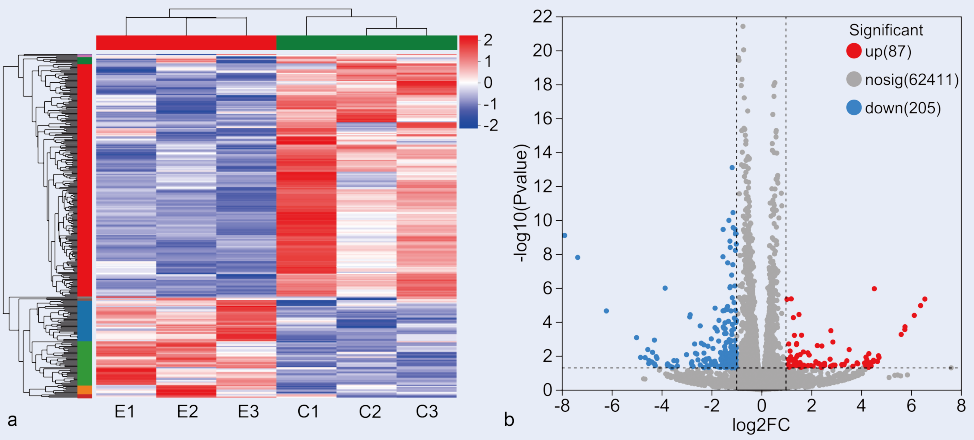


**Figure 3**: **Statistical analysis of differential gene data in the comparison group**. Cluster analysis of DEGs in different groups (**a**). Volcano plot of differential genes (**b**). **Abbreviation:** DEGs (differential expression genes)

DEGs were largely enriched in cell parts, organelles, and membrane components. Regarding MFs, DEGs were primarily linked to binding and catalytic activities.

Mapping DEGs to the KEGG pathway database grouped them into five categories (top 20 pathways shown). In Metabolism (21 DEGs), genes were mainly involved in carbohydrate and lipid metabolism. In Environmental Information Processing (32 DEGs), genes were related to signal transduction and signaling-molecule interactions. In Cellular Processes (21 DEGs), genes concerned cell growth, death, and eukaryotic communities. In Organismal Systems (64 DEGs), genes were involved in the immune, endocrine, and nervous systems. In Human Diseases (69 DEGs), genes were mainly associated with cancer and endocrine and metabolic diseases (**Figure 4b**).

## GO and KEGG functional enrichment analysis of differential genes

GO enrichment identified the 20 most significantly enriched terms, primarily associated with molecular functions (3) and biological processes (17; **Figure 5a**). Five GO terms showed the greatest enrichment: glutamine catabolic process (rich factor = 0.40; 2 DEGs), glutaminase activity (0.40; 2 DEGs), interleukin-21-mediated signaling pathway (0.333; 2 DEGs), glutamate biosynthetic process (0.333; 2 DEGs), and regulation of oocyte maturation (0.333; 2 DEGs).

KEGG enrichment analysis showed that DEGs participated in 208 signaling pathways. The 20 pathways with the most significant enrichment were analyzed (**Figure 5b**); the Ras signaling pathway contained the largest number of enriched genes (**Figure 5c**). The Ras pathway is a crucial intracellular signaling mechanism involved in cell growth, differentiation, apoptosis, and metabolism. Ectoine appears to act by activating receptor tyrosine kinases (RTKs) on the cell surface, triggering downstream cascades that lead to Ras activation. Activated Ras mediates anti-apoptotic effects via the PI3K/Akt pathway: the Ras-PI3K/Akt axis suppresses the AFX transcription factor, thereby down-regulating Fas ligand (FasL) expression, and also promotes NF-$\kappa$B signaling, collectively regulating apoptosis, cell survival, and growth.

## Verification of key DEGs related to skin-cell protection using RT-qPCR

Ectoine treatment markedly enhanced HaCaT cell viability while reducing apoptosis and ROS levels. Based on the transcriptomic data, five key DEGs associated with oxidation, apoptosis, and proliferation were selected for RT-qPCR validation (**Table S4**): MMP25 (extracellular-matrix degradation), NOXO1 (endogenous ROS generation), ANGPTL4 (inflammatory oxidative stress), FOXO6 (pro-apoptotic), and CNFN (keratinocyte structural protein). RT-qPCR showed that ANGPTL4 expression was significantly down-regulated (**Figure 6a**), with lower levels than indicated by RNA-seq. MMP25, NOXO1, and FOXO6 were also significantly down-regulated (**Figure 6b–d**), whereas CNFN was significantly up-regulated (**Figure 6 e**) in ectoine-treated cells, consistent with RNA-seq findings. Overall, RT-qPCR results corroborated the RNA-seq data regarding up-

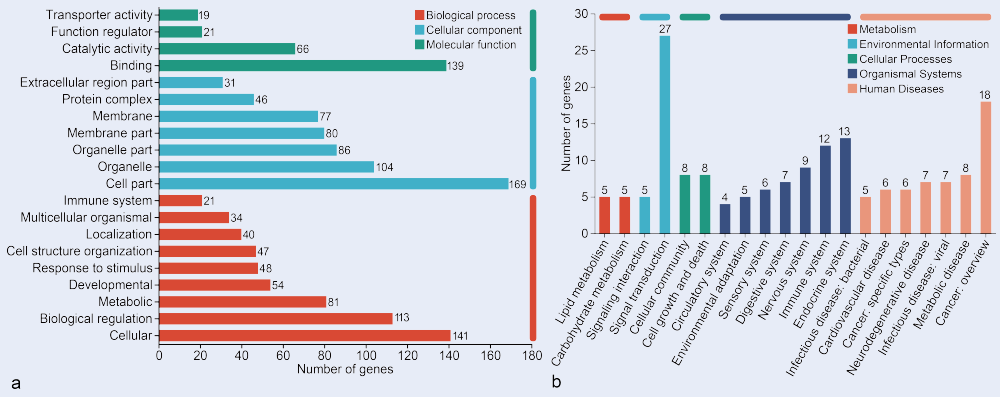


**Figure 4**: **Functional category of DEGs in HaCaT Cells**. GO functional annotation analysis (**a**). KEGG functional annotation analysis (**b**). **Abbreviations**: HaCaT (Human Keratinocytes Cells), DEGs (differential expression genes), GO (Gene Ontology), KEGG (Kyoto Encyclopedia of Genes and Genomes)

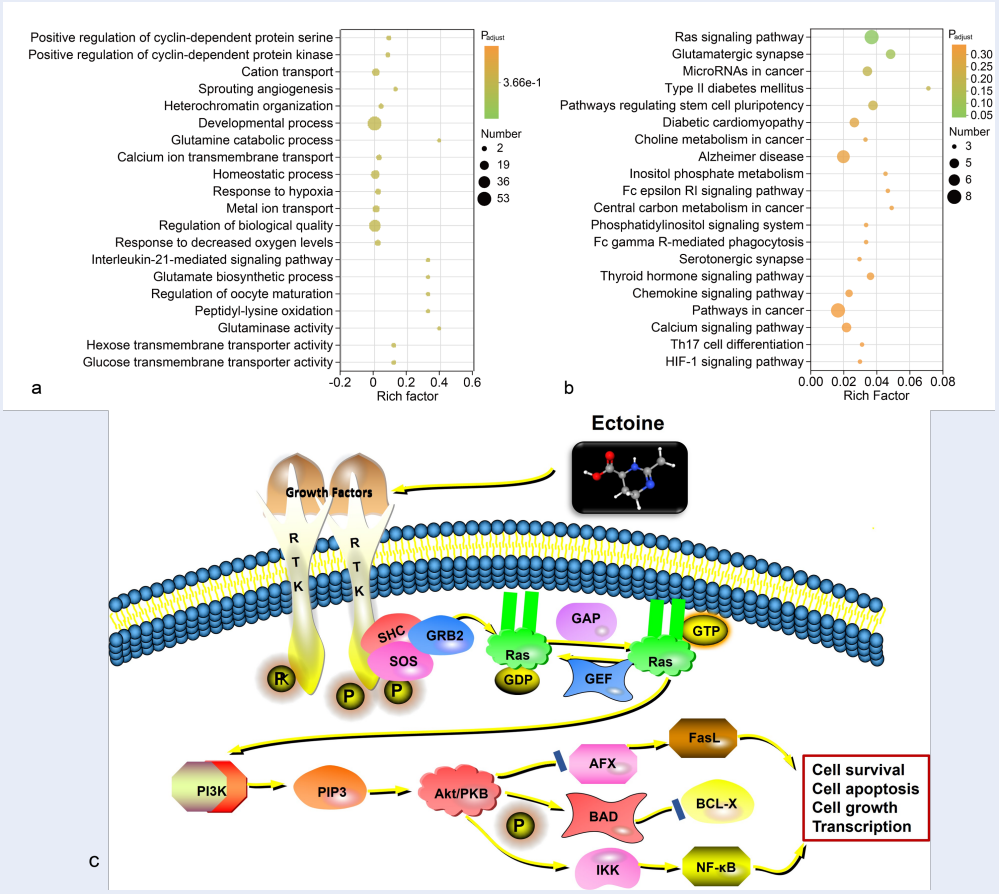


**Figure 5**: **GO and KEGG enrichment analysis of the DEGs**. Bubble chart of GO enrichment analysis (**a**). Bubble chart of KEGG enrichment analysis (**b**). Analysis diagram of the potential mechanism of ectoine regulating the Ras pathway (**c**). **Abbreviations**: DEGs (differential expression genes), DEGs (differential expression genes), GO (Gene Ontology), KEGG (Kyoto Encyclopedia of Genes and Genomes)

and down-regulation patterns (**Figure 6f**). The accuracy of gene-expression quantification can be affected by primer design, instrument sensitivity, and reagent quality.

## DISCUSSION

### Ectoine protects the skin by reducing the apoptosis rate and ROS of HaCaT cells

Apoptosis can be induced by altering the external environment, such as intense UV irradiation and desiccation, by generating ROS. ROS-induced cellular oxidative stress can cause mitochondrial damage, leading to calcium-ion imbalance and inducing the release of apoptotic proteins from the cells, which initiates the process of apoptosis and accelerates the process of skin aging[20,21]. Hseu *et al.*[9] found that after pretreatment of HaCaT cells with ectoine, the expression of antioxidant proteins (HO-1, NQO-1, $\gamma$-GCLC) and the catalytic subunit of $\gamma$-glutamylcysteine ligase ($\gamma$-GCLC) was up-regulated, thereby inhibiting the production of ROS. Cheng *et al.*[10] observed that ectoine alleviated oxidative damage in human skin fibroblasts by up-regulating genes associated with the PI3K/AKT signaling pathway, such as COL1A1, COL1A2, FN1, IGF2, NR4A1 and PIK3R1. In skin cells, NADPH oxidases (NOXs) are endogenous sources of ROS production, while the NOX1 holoenzyme is the main source of ROS produced by ultraviolet (UV) radiation[22]. NOXO1, an essential subunit of NOX1 (encoded by the gene NOXO1), plays a crucial role in activating NOX1 enzymes. ROS also activates signaling pathways that promote the synthesis of matrix metalloproteinases (MMPs)[23,24]. MMP25 is a key gene encoding MMPs, which are enzymes responsible for the degradation of extracellular-matrix (ECM) proteins[25]. ECM proteins are the main connective-tissue component of the dermis[26]. Degradation of the ECM leads to skin laxity and reduced elasticity, which accelerates skin aging and impairs barrier function. In the ectoine experimental group of this study, significant down-regulation of the expression of the gene NOXO1 can reduce the expression of the NOX1 holoenzyme, thus reducing the production of ROS, while significant down-regulation of the expression of the gene MMP25 can decrease the rate of ECM degradation, thereby mitigating ROS-induced damage to skin cells and delaying skin aging. Unlike Hseu *et al.*, who focused on the induction of antioxidant proteins, we identify NOXO1 as a critical target gene of ectoine, demonstrating that its suppression disrupts the assembly of the NOX1 holoenzyme—an effect that directly inhibits ROS generation at an upstream stage rather than scavenging it downstream. While Cheng *et al.* reported that ectoine up-regulates COL1A1 and COL1A2 through the PI3K/AKT pathway, we uncover an additional mechanism by which ectoine down-regulates MMP25 expression, thereby slowing ECM degradation—a previously unrecognized mechanism that contributes to the preservation of skin structural integrity under oxidative stress.

Research has demonstrated that ectoine maintains the integrity of the corneal barrier by inhibiting the pro-inflammatory response and promoting the expression of cytokine IL-37[27]. ANGPTL4 belongs to the family of ANGPTL proteins, which are involved in vasculature generation, inflammation, oxidative stress, vascular permeability and wound healing[28–30]. In a psoriasis study, the gene ANGPTL4 was found to promote inflammatory responses (TNF-$\alpha$, IL-1$\beta$, IL-6 and IL-17A) in keratinocytes by regulating ERK1/2- and STAT3-dependent signaling pathways[31]. Conversely, silencing ANGPTL4 inhibits these effects. Forkhead box protein O6 (FoxO6) is a member of the FoxO family of nuclear transcription factors, which play a crucial role in regulating a diverse array of cellular processes. These processes encompass key functions in cell survival, proliferation, apoptosis, metabolic homeostasis and aging regulation[32], and their target genes include TRAIL (TNF-related apoptosis-inducing ligand), FasL (Fas ligand), Bim (Bcl-2-interacting cell death mediator), pro-apoptotic Bcl-2 family members and Bcl-6[33,34]. Importantly, FoxO6 phosphorylation at Ser184, mediated by Akt, has been shown to promote oxidative stress and inflammation through NF-$\kappa$B activation in keratinocytes[35]. This finding is consistent with our observation that ectoine exerts anti-apoptotic and antioxidant effects by down-regulating FoxO6. Notably, FoxO6 knockdown has been reported to protect ARPE-19 cells from high-glucose-induced ROS accumulation[36] and cardiomyocytes from hypoxia-induced damage[37], further supporting its broad regulatory role in cellular stress responses. In this study, the expression of ANGPTL4 was significantly down-regulated in the ectoine experimental group, suggesting that ectoine inhibits the inflammatory response and thus maintains corneal-barrier integrity. Additionally, the expression of FoxO6 was significantly down-regulated, indicating that ectoine reduces the rate of apoptosis by modulating apoptosis-related transcription factors and by reducing oxidative stress and inflammation.

In this study, 0.2 mg $ml^{-1}$ ectoine significantly reduced the apoptosis rate and ROS levels in HaCaT

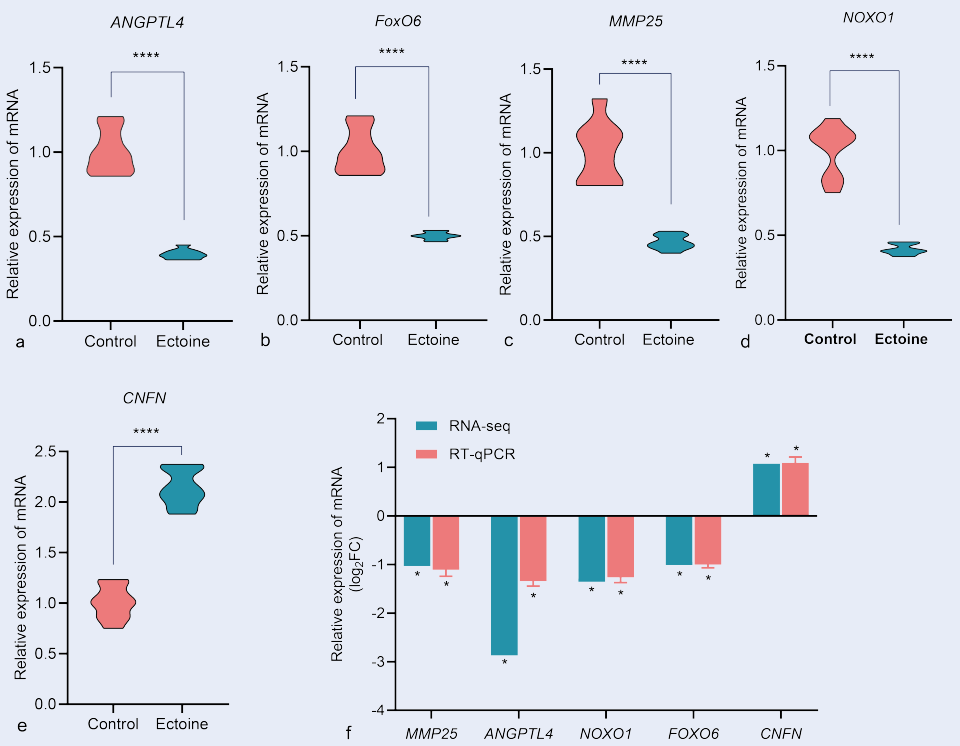


**Figure 6**: **Expression of select genes in Control and ectoine HaCaT cells, data were presented as the mean ± standard error (n = 3/group)**. Comparing the differences in ANGPTL4, FoxO6, MMP25, NOXO1, and CNFN mRNA expression between the cells in each group, the ectoine treatment group was compared with the control group (**a-e**). Compare the results of RT-qPCR with those of RNA-Seq (**f**). **Abbreviation**: ANGPTL4 (Angiopoietin-like 4), FoxO6 (Forkhead box O6), MMP25 (Matrix metallopeptidase 25), NOXO1 (NADPH oxidase organizer 1), and CNFN (Cornifelin), mRNA (Messenger RNA), RT-qPCR (Quantitative reverse transcription polymerase chain reaction), RNA-Seq (RNA sequencing)

cells, and, combined with the transcriptomics results, we speculate that ectoine may protect cells and delay aging by reducing the expression of genes associated with ROS production and apoptosis.

## Ectoine protects skin by enhancing HaCaT cell adhesion

The epidermis is the outermost protective barrier of the human body, and this important barrier function is largely attributed to the differentiation and maturation of keratinocytes and their intercellular-adhesion properties[38]. Ectoine can enhance the mobility of the HaCaT-cell membrane by increasing hydrophilicity and molecular spacing, which in turn enhances the repair mechanism of the membrane and stabilizes the skin barrier[39,40]. Cornifelin (CNFN) has been identified as a protein component of epidermal corneocytes[41]. Liu *et al.*[42] found that CNFN deficiency contributes to cyclic alopecia and impairs the skin's functional barrier in Zdhhc13skc4 mice. Wagner *et al.*[43] found that CNFN deficiency results in defects in keratinocyte desmosome formation, reduced intercellular adhesion and increased susceptibility to damage in the epidermal epithelial layer. In this study, transcription-analysis results indicated that CNFN expression was significantly up-regulated in the experimental group, suggesting that ectoine may increase cell adhesion and connectivity by up-regulating CNFN, thereby enhancing the mechanical stability of cells. This represents a novel finding in elucidating ectoine's skin-repair mechanism.

While this study focused on ectoine's cytoprotective effects in HaCaT cells, we acknowledge the limitation of using a single cell type and propose future research with protein-level validation of key DEGs, multi-cell systems, additional markers of oxidative stress and tissue models to fully characterize its potential in skin-barrier protection, anti-apoptosis, antioxidant activity and other therapeutic applications.

## CONCLUSIONS

Ectoine significantly enhances HaCaT cell viability, reduces oxidative stress and apoptosis, and promotes cell proliferation. Transcriptome analysis revealed that ectoine modulates key genes (MMP25, NOXO1, ANGPTL4, FoXO6, and CNFN) and the RAS pathway, enhancing antioxidative and antiapoptotic effects while strengthening cell adhesion. These findings demonstrate that ectoine protects skin by regulating genes involved in the oxidative response, proliferation, and apoptosis.

## ABBREVIATIONS

**Akt**: Ak strain transforming, **ANGPTL4**: Angiopoietin-like 4, **ANOVA**: Analysis of Variance, **BP**: Biological Process, **C**: Control Group, **CC**: Cellular Component, **CCK-8**: Cell Counting Kit-8, **cDNA**: Complementary DNA, **CNFN**: Cornifelin, **COL1A1**: Collagen Type I Alpha 1 Chain, **COL1A2**: Collagen Type I Alpha 2 Chain, **Ct**: Threshold Cycle, **DCFH-DA**: 2',7'–Dichlorofluorescin diacetate, **DEGs**: Differentially Expressed Genes, **DESeq2**: Differential Gene Expression analysis based on the Negative Binomial distribution, **DMEM**: Dulbecco's Modified Eagle's Medium, **DNA**: Deoxyribonucleic Acid, **E**: Ectoine Group, **ECM**: Extracellular Matrix, **ERK**: Extracellular Signal-Regulated Kinase, **F**: Forward, **FasL**: Fas Ligand, **FBS**: Fetal Bovine Serum, **FC**: Fold Change, **FDR**: False Discovery Rate, **FN1**: Fibronectin 1, **FoxO6**: Forkhead box protein O6, **FPKM**: Fragments Per Kilobase of transcript per Million mapped reads, **gDNA**: Genomic DNA, **GC**: Guanine-Cytosine, **GO**: Gene Ontology, **$\gamma$-GCLC**: Gamma-Glutamyl-Cysteine Ligase Catalytic Subunit, **HaCaT**: Human adult Keratinocyte cell line, **IGF2**: Insulin Like Growth Factor 2, **IL**: Interleukin, **KEGG**: Kyoto Encyclopedia of Genes and Genomes, **MAPK**: Mitogen-Activated Protein Kinase, **MDA**: Malondialdehyde, **MF**: Molecular Function, **MMP**: Matrix Metallopeptidase, **MMP25**: Matrix Metallopeptidase 25, **mRNA**: Messenger RNA, **NF-$\kappa$B**: Nuclear Factor Kappa-Light-Chain-Enhancer of Activated B cells, **NMSC**: Non-Melanoma Skin Cancer, **NOX**: NADPH Oxidase, **NOXO1**: NADPH Oxidase Organizer 1, **NR4A1**: Nuclear Receptor Subfamily 4 Group A Member 1, **Nrf2**: Nuclear Factor Erythroid 2–Related Factor 2, **ns**: Not significant, **PBS**: Phosphate Buffered Saline, **PCR**: Polymerase Chain Reaction, **PI**: Propidium Iodide, **PI3K**: Phosphoinositide 3-Kinase, **PIK3R1**: Phosphoinositide-3-Kinase Regulatory Subunit 1, **POMC**: Pro-Opiomelanocortin, **PPIA**: Peptidylprolyl Isomerase A, **p53**: Tumor protein p53, **R**: Reverse, **RAS**: Rat Sarcoma virus, **RIN**: RNA Integrity Number, **RNA**: Ribonucleic Acid, **RNA-seq**: RNA sequencing, **ROS**: Reactive Oxygen Species, **RT**: Reverse Transcription, **RTKs**: Receptor Tyrosine Kinases, **RT-qPCR**: Quantitative Reverse Transcription Polymerase Chain Reaction, **SD**: Standard Deviation, **STAT3**: Signal Transducer and Activator of Transcription 3, **TNF**: Tumor Necrosis Factor, **TNF-$\alpha$**: Tumor Necrosis Factor Alpha, **TRAIL**: TNF-Related Apoptosis-Inducing Ligand, **TPM**: Transcripts Per Million, **UVA**: Ultraviolet A, **UVB**: Ultraviolet B, **$\alpha$-MSH**: Alpha-Melanocyte-Stimulating Hormone

## ACKNOWLEDGMENTS

None.

## AUTHOR'S CONTRIBUTIONS

Shuo Xu: Formal analysis, Data curation, Data interpretation, Writing-original draft. Peixia Zhang: Supervision, Data analysis. Lijuan Qiao: Supervision. Guoping Shen and Derui Zhu: Bioinformatics technical support. Yongchun Li: Project administration, Funding acquisition. All authors read and approved the final version of the manuscript.

## FUNDING

This research was funded by the Qinghai Science and Technology Department (2024-ZJ-937).

## AVAILABILITY OF DATA AND MATERIALS

Data and materials used and/or analyzed during the current study are available from the corresponding author on reasonable request.

## ETHICS APPROVAL AND CONSENT TO PARTICIPATE

Not applicable.

## CONSENT FOR PUBLICATION

Not applicable.

## DECLARATION OF GENERATIVE AI AND AI-ASSISTED TECHNOLOGIES IN THE WRITING PROCESS

The authors declare that they have not used generative AI (a type of artificial intelligence technology that can produce various types of content in-

cluding text, imagery, audio and synthetic data. Examples include ChatGPT, NovelAI, Jasper AI, Rytr AI, DALL-E, etc) and AI-assisted technologies in the writing process before submission.

## COMPETING INTERESTS

The authors declare that they have no competing interests.

## REFERENCES


1. Rabe JH, Mamelak AJ, McElgunn PJ, Morison WL, Sauder DN. Photoaging: mechanisms and repair. Journal of the American Academy of Dermatology. 2006;55(1):1–19. PMID: 16781287. Available from: https://doi.org/10.1016/j.jaad.2005.05.010.
2. Rieckmann T, Gatzemeier F, Christiansen S, Rothkamm K, Münscher A. The inflammation-reducing compatible solute ectoine does not impair the cytotoxic effect of ionizing radiation on head and neck cancer cells. Scientific Reports. 2019;9(1):6594. PMID: 31036876. Available from: https://doi.org/10.1038/s41598-019-43040-w.
3. Pastor JM, Salvador M, Argandoña M, Bernal V, Reina-Bueno M, Csonka LN. Ectoines in cell stress protection: uses and biotechnological production. Biotechnology Advances. 2010;28(6):782–801. PMID: 20600783. Available from: https://doi.org/10.1016/j.biotechadv.2010.06.005.
4. Abdel-Aziz H, Wadie W, Abdallah DM, Lentzen G, Khayyal MT. Novel effects of ectoine, a bacteria-derived natural tetrahydropyrimidine, in experimental colitis. Phytomedicine : International Journal of Phytotherapy and Phytopharmacology. 2013;20(7):585–91. PMID: 23453305. Available from: https://doi.org/10.1016/j.phymed.2013.01.009.
5. Hahn MB, Meyer S, Schröter MA, Kunte HJ, Solomun T, Sturm H. DNA protection by ectoine from ionizing radiation: molecular mechanisms. Physical Chemistry Chemical Physics : PCCP. 2017;19(37):25717–22. PMID: 28913528. Available from: https://doi.org/10.1039/C7CP02860A.
6. Wittmar J, Meyer S, Sieling T, Kunte J, Smiatek J, Brand I. What Does Ectoine Do to DNA? A Molecular-Scale Picture of Compatible Solute-Biopolymer Interactions. The Journal of Physical Chemistry B. 2020;124(37):7999–8011. PMID: 32816487. Available from: https://doi.org/10.1021/acs.jpcb.0c05273.
7. Fenizia S, Thume K, Wirgenings M, Pohnert G. Ectoine from Bacterial and Algal Origin Is a Compatible Solute in Microalgae. Marine Drugs. 2020;18(1):42. PMID: 31935955. Available from: https://doi.org/10.3390/md18010042.
8. Graf R, Anzali S, Buenger J, Pfluecker F, Driller H. The multifunctional role of ectoine as a natural cell protectant. Clinics in Dermatology. 2008;26(4):326–33. PMID: 18691511. Available from: https://doi.org/10.1016/j.clindermatol.2008.01.002.
9. Hseu YC, Chen XZ, Gowrisankar YV, Yen HR, Chuang JY, Yang HL. The Skin-Whitening Effects of Ectoine via the Suppression of $\alpha$-MSH-Stimulated Melanogenesis and the Activation of Antioxidant Nrf2 Pathways in UVA-Irradiated Keratinocytes. Antioxidants. 2020;9(1):63. PMID: 31936771. Available from: https://doi.org/10.3390/antiox9010063.
10. Cheng W, An Q, Zhang J, Shi X, Wang C, Li M. Protective Effect of Ectoin on UVA/H2O2-Induced Oxidative Damage in Human Skin Fibroblast Cells. Applied Sciences (Basel, Switzerland). 2022;12(17):8531. Available from: https://doi.org/10.3390/app12178531.
11. Kauth M, Trusova OV. Topical Ectoine Application in Children and Adults to Treat Inflammatory Diseases Associated with an Impaired Skin Barrier: A Systematic Review. Dermatology and Therapy. 2022;12(2):295–313. PMID: 35038127. Available from: https://doi.org/10.1007/s13555-021-00676-9.
12. Lin Y, Cao Z, Lyu T, Kong T, Zhang Q, Wu K, et al. Single-cell RNA-seq of UVB-radiated skin reveals landscape of photoaging-related inflammation and protection by vitamin D. Gene. 2022;831:146563. PMID: 35577040. Available from: https://doi.org/10.1016/j.gene.2022.146563.
13. Chen S, Zhou Y, Chen Y, Gu J. fastp: an ultra-fast all-in-one FASTQ preprocessor. Bioinformatics (Oxford, England). 2018;34(17):i884–90. PMID: 30423086. Available from: https://doi.org/10.1093/bioinformatics/bty560.
14. Kim D, Langmead B, Salzberg SL. HISAT: a fast spliced aligner with low memory requirements. Nature Methods. 2015;12(4):357–60. PMID: 25751142. Available from: https://doi.org/10.1038/nmeth.3317.
15. Pertea M, Pertea GM, Antonescu CM, Chang TC, Mendell JT, Salzberg SL. StringTie enables improved reconstruction of a transcriptome from RNA-seq reads. Nature Biotechnology. 2015;33(3):290–5. PMID: 25690850. Available from: https://doi.org/10.1038/nbt.3122.
16. Li B, Dewey CN. RSEM: accurate transcript quantification from RNA-Seq data with or without a reference genome. BMC Bioinformatics. 2011;12(1):323. PMID: 21816040. Available from: https://doi.org/10.1186/1471-2105-12-323.
17. Love MI, Huber W, Anders S. Moderated estimation of fold change and dispersion for RNA-seq data with DESeq2. Genome Biology. 2014;15(12):550. PMID: 25516281. Available from: https://doi.org/10.1186/s13059-014-0550-8.
18. Wang L, Feng Z, Wang X, Wang X, Zhang X. DEGseq: an R package for identifying differentially expressed genes from RNA-seq data. Bioinformatics (Oxford, England). 2010;26(1):136–8. PMID: 19855105. Available from: https://doi.org/10.1093/bioinformatics/btp612.
19. Xie C, Mao X, Huang J, Ding Y, Wu J, Dong S, et al. KOBAS 2.0: a web server for annotation and identification of enriched pathways and diseases. Nucleic acids research. 2011;39(suppl_2):W316–22.
20. Masaki H. Role of antioxidants in the skin: anti-aging effects. Journal of Dermatological Science. 2010;58(2):85–90. PMID: 20399614. Available from: https://doi.org/10.1016/j.jdermsci.2010.03.003.
21. Guo C, Sun L, Chen X, Zhang D. Oxidative stress, mitochondrial damage and neurodegenerative diseases. Neural Regeneration Research. 2013;8(21):2003–14. PMID: 25206509.
22. Glady A, Tanaka M, Moniaga CS, Yasui M, Hara-Chikuma M. Involvement of NADPH oxidase 1 in UVB-induced cell signaling and cytotoxicity in human keratinocytes. Biochemistry and Biophysics Reports. 2018;14:7–15. PMID: 29872728. Available from: https://doi.org/10.1016/j.bbrep.2018.03.004.
23. Kammeyer A, Luiten RM. Oxidation events and skin aging. Ageing Research Reviews. 2015;21:16–29. PMID: 25653189. Available from: https://doi.org/10.1016/j.arr.2015.01.001.
24. Gu Y, Han J, Jiang C, Zhang Y. Biomarkers, oxidative stress and autophagy in skin aging. Ageing Research Reviews. 2020;59. PMID: 32105850. Available from: https://doi.org/10.1016/j.arr.2020.101036.
25. Quan T, Qin Z, Xia W, Shao Y, Voorhees JJ, Fisher GJ. Matrix-degrading metalloproteinases in photoaging. The Journal of Investigative Dermatology Symposium Proceedings. 2009;14(1):20–4. PMID: 19675548. Available from: https://doi.org/10.1038/jidsymp.2009.8.
26. Widgerow AD, Fabi SG, Palestine RF, Rivkin A, Ortiz A, Bucay VW. Extracellular Matrix Modulation: Optimizing Skin Care and Rejuvenation Procedures. Journal of Drugs in Dermatology. 2016;15(4):s63–71. PMID: 27050707.
27. Li JM, Lin N, Zhang Y, Chen X, Liu Z, Lu R. Ectoine protects corneal epithelial survival and barrier from hyperosmotic stress by promoting anti-inflammatory cytokine IL-37. The Ocular Surface. 2024;32:182–91. PMID: 38490477. Available from: https://doi.org/10.1016/j.jtos.2024.03.002.
28. Padua D, Zhang XH, Wang Q, Nadal C, Gerald WL, Gomis RR. TGFbeta primes breast tumors for lung metastasis seeding through angiopoietin-like 4. Cell. 2008;133(1):66–77. PMID: 18394990. Available from: https://doi.org/10.1016/j.cell.2008.01.046.
29. Huang RL, Teo Z, Chong HC, Zhu P, Tan MJ, Tan CK. ANGPTL4 modulates vascular junction integrity by integrin

signaling and disruption of intercellular VE-cadherin and claudin-5 clusters. Blood. 2011;118(14):3990–4002. PMID: 21841165. Available from: https://doi.org/10.1182/blood-2011-01-328716.

30. Goh YY, Pal M, Chong HC, Zhu P, Tan MJ, Punugu L. Angiopoietin-like 4 interacts with matrix proteins to modulate wound healing. The Journal of Biological Chemistry. 2010;285(43):32999–3009. PMID: 20729546. Available from: https://doi.org/10.1074/jbc.M110.108175.
31. Zuo Y, Dai L, Li L, Huang Y, Liu X, Liu X, et al. ANGPTL4 Regulates Psoriasis via Modulating Hyperproliferation and Inflammation of Keratinocytes. Frontiers in Pharmacology. 2022;13:850967. PMID: 35860030. Available from: https://doi.org/10.3389/fphar.2022.850967.
32. Zhang M, Zhang X. The role of PI3K/AKT/FOXO signaling in psoriasis. Archives of Dermatological Research. 2019;311(2):83–91. PMID: 30483877. Available from: https://doi.org/10.1007/s00403-018-1879-8.
33. Birkenkamp KU, Coffer PJ. Regulation of cell survival and proliferation by the FOXO (Forkhead box, class O) subfamily of Forkhead transcription factors. Biochemical Society Transactions. 2003;31(Pt 1):292–7. PMID: 12546704. Available from: https://doi.org/10.1042/bst0310292.
34. Burgering BM, Medema RH. Decisions on life and death: FOXO Forkhead transcription factors are in command when PKB/Akt is off duty. Journal of Leukocyte Biology. 2003;73(6):689–701. PMID: 12773501. Available from: https://doi.org/10.1189/jlb.1202629.
35. Bang E, Kim DH, Chung HY. Protease-activated receptor 2 induces ROS-mediated inflammation through Akt-mediated NF-κB and FoxO6 modulation during skin photoaging. Redox Biology. 2021;44:102022. PMID: 34082382. Available from: https://doi.org/10.1016/j.redox.2021.102022.
36. Zhou Z, Liu J, Bi C, Chen L, Jiao Y, Cui L. Knockdown of FOXO6 inhibits high glucose-induced oxidative stress and apoptosis in retinal pigment epithelial cells. Journal of Cellular Biochemistry. 2019;120(6):9716–23. PMID: 30548643. Available from: https://doi.org/10.1002/jcb.28252.
37. Jin A, Zhang Q, Li S, Li B. Downregulation of FOXO6 alleviates hypoxia-induced apoptosis and oxidative stress in cardiomyocytes by enhancing Nrf2 activation via upregulation of SIRT6. Journal of Bioenergetics and Biomembranes. 2020;52(6):409–19. PMID: 33123950. Available from: https://doi.org/10.1007/s10863-020-09856-2.
38. Sumigray KD, Lechler T. Cell adhesion in epidermal development and barrier formation. Current Topics in Developmental Biology. 2015;112:383–414. PMID: 25733147. Available from: https://doi.org/10.1016/bs.ctdb.2014.11.027.
39. Harishchandra RK, Wulff S, Lentzen G, Neuhaus T, Galla HJ. The effect of compatible solute ectoines on the structural organization of lipid monolayer and bilayer membranes. Biophysical Chemistry. 2010;150(1-3):37–46. PMID: 20206435. Available from: https://doi.org/10.1016/j.bpc.2010.02.007.
40. Dwivedi M, Brinkkötter M, Harishchandra RK, Galla HJ. Biophysical investigations of the structure and function of the tear fluid lipid layers and the effect of ectoine. Part B: artificial lipid films. Biochimica et Biophysica Acta. 2014;1838(10):2716–27. PMID: 24853656. Available from: https://doi.org/10.1016/j.bbamem.2014.05.007.
41. Michibata H, Chiba H, Wakimoto K, Seishima M, Kawasaki S, Okubo K. Identification and characterization of a novel component of the cornified envelope, cornifelin. Biochemical and Biophysical Research Communications. 2004;318(4):803–13. PMID: 15147942. Available from: https://doi.org/10.1016/j.bbrc.2004.04.109.
42. Liu KM, Chen YJ, Shen LF, Haddad AN, Song IW, Chen LY. Cyclic Alopecia and Abnormal Epidermal Cornification in Zdhhc13-Deficient Mice Reveal the Importance of Palmitoylation in Hair and Skin Differentiation. The Journal of Investigative Dermatology. 2015;135(11):2603–10. PMID: 26121212. Available from: https://doi.org/10.1038/jid.2015.240.
43. Wagner T, Beer L, Gschwandtner M, Eckhart L, Kalinina P, Laggner M, et al. The Differentiation-Associated Keratinocyte Protein Cornifelin Contributes to Cell-Cell Adhesion of Epidermal and Mucosal Keratinocytes. The Journal of Investigative Dermatology. 2019;139(11):2292–2301.e9. PMID: 31129056. Available from: https://doi.org/10.1016/j.jid.2019.04.019.